The design of erbium-doped fiber amplifiers

Pedersen, Bo; Bjarklev, Anders Overgaard; Povlsen, Jørn Hedegaard; Dybdal, Kristen; Larsen, Carl Christian

Published in:
Journal of Lightwave Technology

Link to article, DOI:
10.1109/50.85807

Publication date:
1991

Document Version
Publisher's PDF, also known as Version of record

The Design of Erbium-Doped Fiber Amplifiers

Bo Pedersen, Anders Bjarklev, Jørn Hedegaard Povlsen, Kristen Dybdal, and Carl Christian Larsen

Abstract—**An accurate model for the erbium-doped fiber amplifier is presented. The model is used to design the index profile of the doped fiber, optimizing with regard to efficiency for in-line- and preamplifiers as well as for power booster amplifiers. The predicted pump efficiencies (maximum gain to pump power ratios) are in very good agreement with experimental results presented in the international literature. The choice of codopant is shown to be very significant for the pump efficiency when pumping at 0.98 μm. The pump efficiency in the 0.98-μm pump band is shown to be twice the pump efficiency in the 1.48-μm pump band.**

I. Introduction

LIGHT amplification in rare earth's doped fibers has been studied for a long time [1]. Recently, the erbium-doped fiber amplifier (EDFA) has been shown to be a potential alternative to the semiconductor laser amplifier, operating in the third communication window for optical fiber systems [2]–[5]. As compared to the semiconductor laser amplifier, the advantage of using an EDFA includes high gain [3], [4], high saturation output power [5], polarization independent gain [6], no crosstalk [7], low noise figure [2], and low insertion loss. The EDFA can be pumped at several wavelengths. However, for practical optical fiber communication systems, the EDFA must be pumped by semiconductor laser diodes. Therefore, the most interesting pump wavelengths are at 0.81, 0.98, and 1.48 μm. The excited state absorption in the 0.81-μm pump band [8] implies a high pump power to achieve a high gain [9]. A high pump power causes a low lifetime for the pump laser. The latest reports of high gain achieved with low pump power in the 0.98 and 1.48-μm pump bands [10]–[12] has therefore stimulated the interest for these two pump bands.

The focus of this paper is the design of EDFA's including a comparison of the 0.98 and 1.48-μm pump band. Also, the erbium-doped fibers with germanium, used as index raising codopant, (Ge/Er-fibers) will be compared to erbium-doped fibers with aluminum, used as index raising codopant (Al/Er-fibers). A comprehensive model is presented and used to optimize the performance of the EDFA used as in-line- and preamplifiers as well as power booster amplifiers. The cross sections used by the model have carefully been evaluated by measurements on an Al/Er- and a Ge/Er-fiber.

II. Theory

The erbium-ion is described with the energy level diagram shown in Fig. 1. When pumping at 0.98 μm the EDFA acts as a 3-level laser system which means that the Er^{3+}-ion is excited from the ground state level, $^4I_{15/2}$, to a third level, $^4I_{11/2}$, from which it rapidly decays to the upper laser level, $^4I_{13/2}$. This raises the possibility of a complete inversion in the upper laser level. When pumping at 1.48 μm the Er^{3+}-ion is excited directly into the upper laser level, which means that the EDFA acts as 2-level laser system and that the inversion, n_2 in the upper laser level cannot pass a value $n_2^{\max}$ set by the emission to absorption cross-section ratio, $\epsilon = \sigma_{pe}/\sigma_{pa}$, at 1.48 μm:

$$n_2^{\max} = \frac{1}{1+\epsilon}. \tag{1}$$

The EDFA is described in a (r, ϕ, z)-cylindrical coordinate system with the z axis as fiber axis. Considering only LP_{01}-modes and a circular symmetry for the EDFA, the steady-state population concentrations, $N_1(r, z)$ and $N_2(r, z)$, in the ground and excited state, respectively, are evaluated from the transition rates of the pump, signal and spontaneous emission

$$N_2(r, z) = \rho_{\mathrm{Er}}(r)\frac{R_{\mathrm{pe}}(r, z) + W_{\mathrm{se}}(r, z) + A_e}{R_{\mathrm{pe}}(r, z) + R_{\mathrm{pa}}(r, z) + W_{\mathrm{se}}(r, z) + W_{\mathrm{sa}}(r, z) + A_e} \tag{2}$$

$$N_1(r, z) = \rho_{\mathrm{Er}}(r) - N_2(r, z) \tag{3}$$

where $\rho_{\mathrm{Er}}(r)$ is the erbium concentration and $A_e = 1/\tau_e$ is the spontaneous emission rate, τ_e being the lifetime. The transition rates are determined as follows. The pump absorption rate

$$R_{\mathrm{pa}}(r, z) = \sigma_{\mathrm{pa}} \cdot \frac{P_p(z)}{h\nu_p} I_p^{01}(r) \tag{4}$$

Manuscript received November 5, 1990; revised May 9, 1991. This work was supported in part by the Danish Technical Research Council.

B. Pedersen, A. Bjarklev, and J. H. Porlsen are with the Technical University of Denmark, Electromagnetics Institute, Center for Broadband Telecommunications, DK-2800 Lyngby, Denmark.

K. Dybdal is with Jydsk Telefon, Sletvej 30, 8310 Tranbjerg, Denmark.

C. C. Larsen is with Lycom A/S, NKT Alle75, 2605 Brøndby, Denmark.

IEEE Log Number 9101621.

0733-8724/91/0900-1105$01.00 © 1991 IEEE

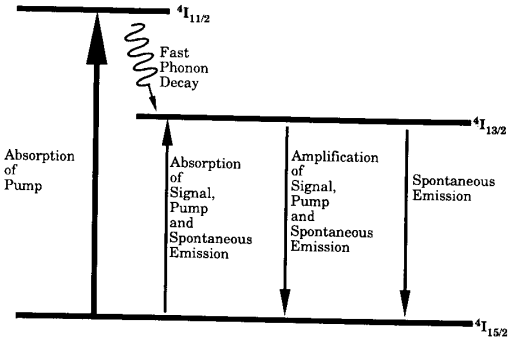

Fig. 1. Relevant energy levels for erbium.

where σ_{pa} is the absorption cross section at the pump wavelength, $P_p(z)$ is the pump power at position z in the fiber, h is Planck's constant, ν_p is the pump frequency, and $I_p^{01}(r)$ is the normalized LP_{01}-mode, $2\pi\int_0^\infty I^{01}(r)r\,dr = 1$, at the pump wavelength.

The pump emission rate is considered only when pumping at 1.48 μm

$$R_{pe}(r, z) = \sigma_{pe} \cdot \frac{P_p(z)}{h\nu_p} I_p^{01}(r) \tag{5}$$

where σ_{pe} is the emission cross section at 1.48 μm. For 0.98 μm pumping σ_{pe} is zero and consequently $R_{pe}(r, z)$ in (2) is zero.

The signal emission and absorption rates, W_{se} and W_{sa}, are calculated from the signal and the amplified spontaneous emission

$$W_{se}(r, z) = \left[\frac{\sigma_e(\nu_s)}{h\nu_s} P_s(z) + \int_0^\infty \frac{\sigma_e(\nu)}{h\nu} \cdot S_{ASE}(\nu, z)\, d\nu\right] I_s^{01}(r) \tag{6}$$

$$W_{sa}(r, z) = \left[\frac{\sigma_a(\nu_s)}{h\nu_s} P_s(z) + \int_0^\infty \frac{\sigma_a(\nu)}{h\nu} \cdot S_{ASE}(\nu, z)\, d\nu\right] I_s^{01}(r) \tag{7}$$

where $\sigma_e(\nu)$ and $\sigma_a(\nu)$ are the emission and absorption cross sections, respectively, at the frequency ν. ν_s is the signal frequency, $S_{ASE}(\nu, z)$ is the amplified spontaneous emission power spectral density at the position z.

The spontaneous emission is amplified in both the forward and the backward direction of the fiber axis. This means that the total amplified spontaneous emission spectrum, $S_{ASE}(\nu, z)$ used in (6), (7) has to be determined from a forward as well as a backward traveling amplified spontaneous emission spectrum, $S_{ASE}^+(\nu, z)$ and $S_{ASE}^-(\nu, z)$

$$S_{ASE}(\nu, z) = S_{ASE}^+(\nu, z) + S_{ASE}^-(\nu, z). \tag{8}$$

The differential equations for propagation of $S_{ASE}^+(\nu, z)$ and $S_{ASE}^-(\nu, z)$ are given by

$$\frac{dS_{ASE}^-(\nu, z)}{dz} = -2h\nu\gamma_e(\nu, z) - [\gamma_e(\nu, z) - \gamma_a(\nu, z)] \cdot S_{ASE}^-(\nu, z) \tag{9}$$

and

$$\frac{dS_{ASE}^+(\nu, z)}{dz} = +2h\nu\gamma_e(\nu, z) + [\gamma_e(\nu, z) - \gamma_a(\nu, z)] \cdot S_{ASE}^+(\nu, z) \tag{10}$$

where the emission-, $\gamma_e(\nu, z)$, and absorption-, $\gamma_a(\nu, z)$, factors are determined from the emission and absorption cross sections, respectively, and the overlap integral between the signal mode and the population concentration in the excited and the ground state, respectively

$$\gamma_e(\nu, z) = \sigma_e(\nu) \cdot 2\pi \int_0^{a_d} N_2(r, z) I_s^{01}(r) r\, dr \tag{11}$$

$$\gamma_a(\nu, z) = \sigma_a(\nu) \cdot 2\pi \int_0^{a_d} N_1(r, z) I_s^{01}(r) r\, dr \tag{12}$$

where a_d is the erbium-doping radius. The signal is amplified, in the positive direction of the fiber axis, according to

$$\frac{dP_s(z)}{dz} = [\gamma_e(\nu_s, z) - \gamma_a(\nu_s, z)]P_s(z). \tag{13}$$

The pump is propagating in the forward direction of the fiber

$$\frac{dP_p(z)}{dz} = [\gamma_e(\nu_p, z) - \gamma_a(\nu_p, z)]P_p(z) \tag{14}$$

where the pump emission-, $\gamma_e(\nu_p, z)$, and absorption-, $\gamma_a(\nu_p, z)$, factors are determined from equations similar to (11) and (12), just using the cross sections at the pump wavelength as well as the pump LP_{01}-mode, $I_p^{01}(r)$. For 0.98 μm pumping $\gamma_e(\nu_p, z)$ is zero.

The noise figure F, of an EDFA is defined with respect to the idealized case of a coherent input signal and an infinitesimal receiver bandwidth around the optical frequency of the signal. In Appendix A it is that the quantity $(F \cdot G - 1)/h\nu_s$, where G is the gain and $h\nu_s$ the energy of a signal photon, obeys the same differential equation as $S_{ASE}^+(\nu, z)$ in (10). Since both $F \cdot G$-1 and $S_{ASE}^+(\nu, z)$ vanish at $z = 0$, the noise figure can be expressed as

$$F = (S_{ASE}^+(\nu_s, L)/h\nu_s + 1)/G. \tag{15}$$

The noise figure can accordingly be interpreted as a measure of the spectral density of the ASE around the signal frequency.

An alternative formula for F [14] says:

$$F = \int_0^L \frac{\gamma_e(\nu_s, z) + \gamma_a(\nu_s, z)}{P_s(z)} \cdot P_s(0)\, dz + 1 \tag{16}$$

from which it can be seen that the more rapid the gain increases in the beginning of the EDFA the lower becomes the F and thereby also, from (15), the $S_{ASE}^+(\nu_s, L)$.

III. Determination of Cross Sections

The Stark splitting of the energy levels in erbium yields the wavelength dependent emission and absorption cross section, $\sigma_e(\nu)$ and $\sigma_a(\nu)$, respectively, used in the description of the transitions between level $^4I_{15/2}$ and level $^4I_{13/2}$. If no erbium ions are excited the absorption cross sections can be determined directly from an attenuation measurement using (13)

$$\sigma_a(\nu) = \frac{\text{att}\ (\nu)}{10 \log_{10}(e) \cdot 2\pi \int_0^{a_d} \rho_{\text{Er}}(r) I^{01}(\nu, r) r\, dr} \tag{17}$$

where att (ν) is the attenuation in dB/m, at the frequency ν.

The emission cross sections can be determined from a gain measurement, implied that all erbium ions are excited

$$\sigma_e(\nu) = \frac{g(\nu)}{10 \log_{10}(e) \cdot 2\pi \int_0^{a_d} \rho_{\text{Er}}(r) I^{01}(\nu, r) r\, dr} \tag{18}$$

where $g(\nu)$ is the gain, in dB/m, at frequency ν.

Determination of the cross sections, using (17) and (18), implies an accurate knowledge of the overlap integral between the erbium concentration and the LP_{01} mode. However, the emission cross sections can also be determined from the spectral shape of the fluorescence, $I_e(\nu)$, and the spontaneous emission rate A_e. The following equation can be derived from the Fuchtbauer–Ladenburg equations [15]:

$$\sigma_e(\nu) = \frac{A_e \lambda^2}{8\pi n^2} \frac{I_e(\nu)}{\int I_e(\nu)\, d\nu} \tag{19}$$

where n is the refractive index and λ is an average wavelength.

In Fig. 2 is shown the emission cross section versus wavelength, as determined from (19), for both an Al/Er-fiber (solid) and a Ge/Er-fiber (dashed). The spectral shape function, $I_e(\nu)$, were measured on very short fibers pumped with high power. The measured spontaneous lifetime, $\tau_e = 1/A_e$, were 10.6 and 12.5 ms for the Al/Er-fiber and the Ge/Er-fiber, respectively.

In the upper right corner in Fig. 2 is shown the measured gain versus fiber length for an Al/Er-fiber, pumped with 115 mW at 654 nm. The signal wavelength is 1.530 μm. As seen from this measurement the slope approaches 2.13 dB/m when the fiber length decreases toward zero. Assuming that a complete inversion is obtained at shorter fiber length, the overlap integral between the erbium concentration and the signal LP_{01} mode is determined, using (18), to be 9.81×10^{23} m^{-3}. This estimated overlap, that assumes that the emission cross section found from (19) is valid, is in very good agreement with the overlap of 9.35×10^{23} m^{-3} estimated directly from the calculated LP_{01} mode and the erbium concentration profile which was

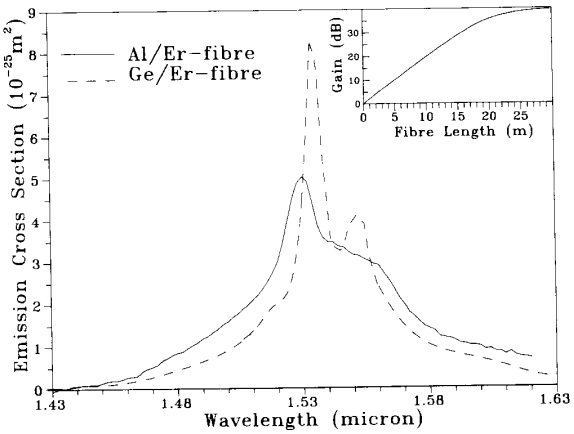

Fig. 2. Emission cross section versus wavelength in erbium-doped fiber codoped with aluminum (solid) and germanium (dashed). Upper right figure: Measured gain versus fiber length in Al/Er-fiber pumped with 115 mW at 0.654 μm. The signal wavelength is 1.530 μm.

measured with a scanning electron microprobe. The later overlap is estimated to be accurate to within 10% which was the accuracy of the microprobe calibration.

The attenuation at 1.530 μm for the fiber was measured to be 2.14 dB/m. From (17) and (18) it is seen that the ratio of the emission to absorption cross section is equal to the ratio of $g(\nu)$ to att (ν). Since $g(\nu)$ and att (ν) was measured to be equal at 1.530 μm, the absorption cross section must be equal to the emission cross section at 1530 nm. Consequently, the absorption cross-section spectrum can be found by scaling the attenuation spectrum to the known cross section at 1530 nm. The scaled absorption cross-section spectrum is shown (solid curve) in Fig. 3. It should be noted that when determining the emission to absorption cross-section ratio directly from a gain to attenuation ratio measurement it is of high importance the gain measurement is performed on a short fiber to avoid saturation due to ASE. Also the pump power most be high enough to fully invert all Er^{3+}-ions in the fiber. Furthermore, the fiber must be so ideal that no intrinsic losses deteriorate the measurements. If any of these three assumptions are not valid the estimated ratio will be smaller than the true ratio. The authors are convinced that all three assumptions were fulfilled in the measurement, and we find confidence in the fact that the estimated ratio of unity is, to our knowledge, slightly higher than what has been published by other authors using the same technique.

The absorption cross-section spectrum can also be determined from the spectral shape of the attenuation, $I_a(\nu)$, according to the Fuchtbauer–Ladenburg equations

$$\sigma_a(\nu) = \frac{A_e \lambda^2}{8\pi n^2} \frac{2J_2 + 1}{2J_1 + 1} \frac{I_a(\nu)}{\int I_a(\nu)\, d\nu} \tag{20}$$

where J_1 and J_2 are the angular momentum quantum numbers for the ground and the excited state, respectively.

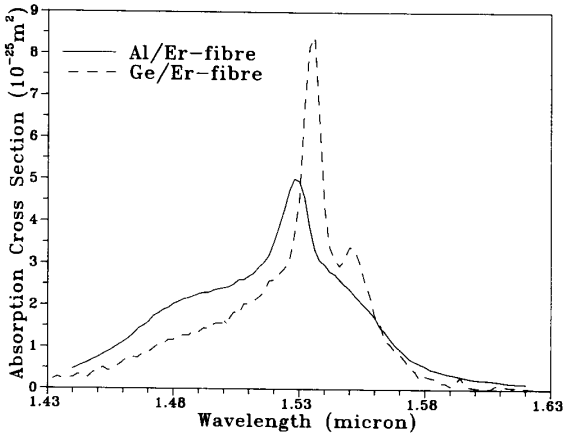

Fig. 3. Emission cross section versus wavelength in erbium-doped fiber codoped with aluminum (solid) and germanium (dashed).

If the absorption cross-section spectrum is evaluated from (20), the resulting cross sections will be 15% lower than the values determined from (17). The validity of the Fuchtbauer–Ladenburg equations has been questioned by other authors [16], [17]. In [17], it is shown that the absorption cross sections, found from (20) in Ge/Er-preforms, are 10 to 20% too low. In Fig. 3, the dashed curve represents the absorption cross-section spectrum for a Ge/Er-fiber, found from the measured attenuation spectrum, using (20) and a correction of 1.15. The cross sections, shown in Figs. 2 and 3, are the cross sections used in the following calculations.

The absorption cross section of 2.0×10^{-25} m^2 at 0.98 μm for the Al/Er-fiber was found from attenuation measurements on a well-characterized fiber from which very good agreement between model predictions, using the model presented here, and measured properties in the small signal region has been found [18]. For the Ge/Er-fiber an absorption cross section as high as 4.5×10^{-25} m^2 was found. When estimating the absorption cross sections at 0.98 μm for the two fibers it was assumed that the erbium concentration profile follows the profile of the refractive index in the fiber. The excellent agreement between measurements and model predictions [18] indicate that this assumption is valid for Al/Er-fibers and therefore the error in the predicted absorption cross section at 0.98 μm for the Al/Er-fiber is estimated to be less than 10%. However, the model has not been verified for a Ge/Er-fiber and the predicted cross section is more uncertain for this fiber.

IV. Numerical Solution

The LP_{01}-modes at the pump and the signal wavelength are determined from a multilayer model [19] and can be calculated from an arbitrary circular symmetric refractive-index profile.

The forward and the backward amplified spontaneous emission are both presented in 200 frequency slots from $\lambda = 1.43$ to 1.63 μm. The resulting spacing of 1 nm is found necessary when calculating with the spectra from the Ge/Er-fiber. These spectra are the most critical because the linewidth of the peaks are more narrow than for the spectra from the Al/Er-fiber. Equations (9), (10), (13), and (14) yield 402 coupled differential equations which are solved by numerical integration through the fiber. In each step the overlap integrals involved in (11) and (12) and the similar equations for γ_{pe} and γ_{pa} are solved numerically by representing $I_s^{01}(r)$ and $I_p^{01}(r)$ in 40 equidistant points from $r = 0$ to $r = a_d$. $N_2(r, z)$ are evaluated from (2)–(7) in the same 40 points for each step in the fiber.

The backward ASE introduces a two boundary problem which leads to the necessity of iterative forward and backward integrations in the fiber. The iteration is started with a forward integration, from $z = 0$, of the signal, the pump, and the forward ASE, in which the backward ASE is zero. After this, each backward integration is started, at $z = L$, with the results $P_S(L)$, $P_p(L)$ and $S^+_{ASE}(\nu_n, L)$, from the previous forward integration, together with the boundary condition, $S^-_{ASE}(\nu_n, L) = 0$, as starting conditions. Analogously, the starting conditions at $z = 0$ for each forward integration are the results of the previous integration as guess for $S^-_{ASE}(\nu, 0)$ and the boundary conditions, $S^+_{ASE}(\nu_n, 0) = 0$, $P_p(0)$ = input pump power and $P_s(0)$ = input signal power. The iteration is stopped when the gain, in decibels, from the two latest forward integrations deviate with less than 10^{-7}%. This rather strong criterion has been found necessary, when the length for maximum gain has to be found. Furthermore, fulfilling this criterion for the gain ensures that the analogous criteria for the ASE and the pump power are also fulfilled.

The number of iterations varies from 5 to 30 dependent on the actual conditions, type of fiber, fiber length, pump and signal power, and pump and signal wavelength.

To insure consistency, both (15) and (16) are solved numerically, giving the same noise figure F, for the EDFA.

V. Refractive Index and Erbium Concentration Profiles

Considering step-index profiles for both refractive index, $n(r)$, and erbium concentration, $\rho_{Er}(r)$

$$n(r) = \begin{cases} n_1, & r \le a_k \\ n_2, & r > a_k \end{cases} \text{ and } \rho_{Er}(r) = \begin{cases} \rho^0_{Er}, & r \le a_k \\ 0, & r > a_k \end{cases} \tag{21}$$

where n_1 and n_2 are the refractive index in, respectively, the core and cladding, ρ^0_{Er} is the erbium concentration and a_k is the core and doping radius. In the following the erbium-doped fiber is characterized as a function of the cutoff wavelength λ_c, for the LP_{11}-mode and the numerical aperture, NA $= \sqrt{n_1^2 - n_2^2}$. The erbium concentration does not appear in the results of this contribution, because all fiber lengths are optimized with regard to maximum gain.

VI. In-Line-Amplifiers and Preamplifiers

When the EDFA is used as in-line- or as preamplifier the signal is so low that the amplifier is in the unsaturated region. When designing the EDFA in this region, the goal is to achieve the highest gain for an available pump power or to minimize the pump power needed for a specified gain. The latest goal is posed because a smaller pump power results in a longer lifetime for the pump laser, which is very important when the EDFA is used in a commercial optical communication system.

In the following, the pump efficiency is used to characterize the fulfillment of the two goals posed here. The pump efficiency is defined as the maximum ratio between gain in decibels and launched pump power in milliwatts. The procedure for finding the pump efficiency for a given fiber design is to iteratively change the pump power, optimizing the fiber length with regard to small signal gain and compute the gain to pump power ratio, until the maximum ratio is achieved.

In Fig. 4 the pump efficiency is shown versus cutoff wavelength, λ_c, for the LP_{11}-mode in a step-index Al/Er-fiber. Curves for NA = 0.1 to NA = 0.4 in steps of 0.05 are shown for both 0.98 μm (solid) and 1.48 μm (dashed) pumping. The signal wavelength is 1.53 μm. As seen from the figure the pump efficiency for a given NA has a maximum with regard to cutoff wavelength. This optimum cutoff wavelength is independent of the NA. For 0.98 μm and for 1.48-μm pumping the optimum cutoff wavelength is 0.80 and 0.90 μm, respectively.

The pump efficiency at the optimum cutoff wavelength is shown versus NA in Fig. 5. The solid curves represent results for Al/Er-fibers and are obtained from Fig. 4. The dashed curves represent results for Ge/Er-fibers, computed with a signal wavelength of 1.535 μm. Curves for 1.48 μm (marks) as well as for 0.98 μm pumping is presented. As seen from Fig. 5 the highest pump efficiency is obtained in EDFA's codoped with germanium and pumped at 0.98 μm. The absorption cross section at 0.98 μm in Ge/Er-fibers was estimated to be more than twice the value in Al/Er-fibers. Also the emission peak in the Ge/Er-fibers is approximately 60% higher than the peak in the Al/Er-fibers (see Fig. 2). This explains why the pump efficiency is predicted to be up to 12 dB/mW higher in Ge/Er-fibers than in Al/Er-fibers, when pumping at 0.98 μm. At 1.48-μm pumping the pump efficiency in Ge/Er-fibers is up to 1.3 dB/mW higher than in Al/Er-fibers. The maximum obtainable inversion, see (1), in the upper laser level, when pumping at 1.48 μm, is 70% for both Al/Er- and Ge/Er-fibers, but the absorption cross section at 1.48 μm in Al/Er-fibers is twice the value in Ge/Er-fibers. This is the reason why the advantage, with regard to pump efficiency, in using Ge/Er-fibers is not so significant when pumping at 1.48 μm as when pumping at 0.98 μm.

In [12] is presented experimental results of pump efficiency in Ge/Er-fibers with different NA pumped at 0.98 μm. The obtained pump efficiencies agree very well with the pump efficiencies presented in Fig. 5. The Ge/Er-fiber, from [12], with the highest NA of 0.28 was pumped at 1.48 μm as well as at 0.98 μm and the obtained pump efficiencies was 5.0 and 11.0 dB/mW, respectively. The curves in Fig. 5 yields 4.3 and 11.8 dB/mW.

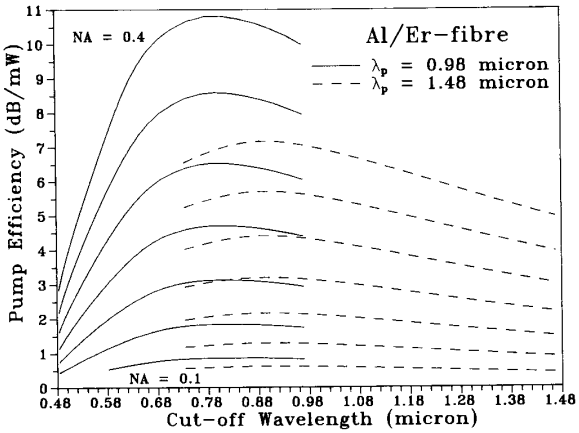

Fig. 4. Pump efficiency, i.e., maximum ratio between small signal gain in decibels and pump power in milliwatts versus cutoff wavelength for step index Al/Er-fiber pumped at 0.98 μm (solid) and 1.48 μm (dashed). The numerical aperture (NA) is change from 0.1 to 0.4 in steps of 0.05.

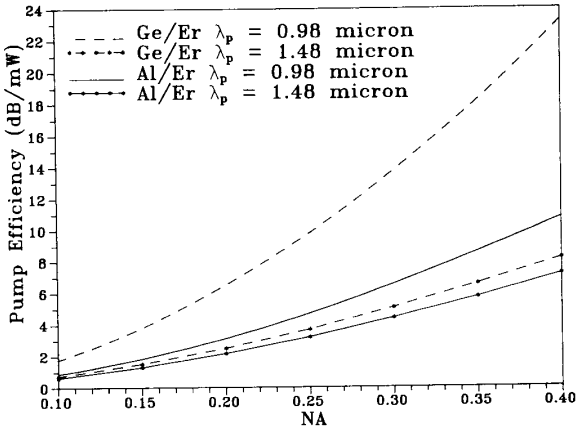

Fig. 5. Maximum pump efficiency versus numerical aperture (NA) in step-index Ge/Er-fibers (dashed) and Al/Er-fibers (solid), pumped at 1.48 μm (marks) and at 0.98 μm.

In Fig. 6 is shown the pump powers resulting in the pump efficiencies shown in Fig. 5 versus NA. As seen from Fig. 6 the advantage, with respect to lower required pump power, in using a higher NA is most pronounced when the NA is small. Furthermore, the 0.98-μm pump band does not require as much pump power as the 1.48-μm pump band.

The noise figures, at the pump efficiencies from Fig. 5, is shown in Fig. 7 versus NA. As seen from Fig. 7, the Al/Er-fiber and the Ge/Er-fiber has almost identical noise figure, when pumping at 0.98 μm. For 1.48-μm pumping, the noise figure for the Ge/Er-fiber is 1.8 dB higher than for the Al/Er-fiber.

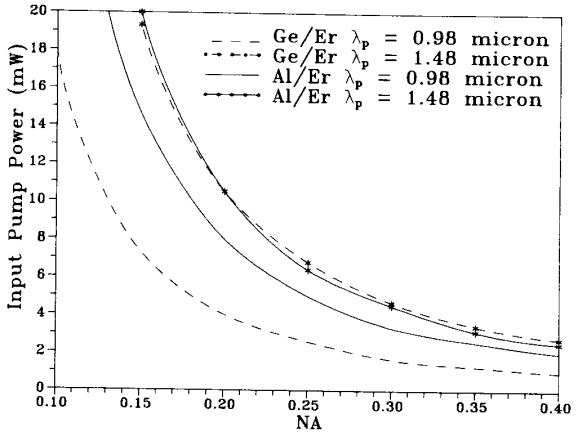

Fig. 6. Pump power, giving the maximum pump efficiency, versus numerical aperture (NA) in step-index Ge/Er-fibers (dashed) and Al/Er-fibers (solid), pumped at 1.48 μm (marks) and at 0.98 μm.

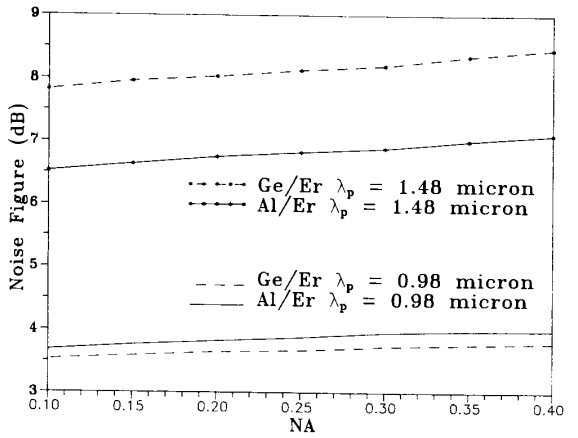

Fig. 7. Noise figure, when maximum pump efficiency is obtained, versus numerical aperture (NA) in step-index Ge/Er-fibers (dashed) and Al/Er-fibers (solid), pumped at 1.48 μm (marks) and at 0.98 μm.

The above presented results permit the conclusion that the 0.98 μm pumped Ge/Er-fiber should be used as in-line- and preamplifier. However, assuming 1.48 μm pumping, it is not significant for the pump efficiency whether to use germanium or aluminum as codopant.

Furthermore, trial calculations with other profiles has shown that the step index profile is the optimum profile, regarding to pump efficiency, assuming equal NA.

VII. Power Booster Amplifiers

When using the EDFA as power booster, the signal at the input is relatively high. The maximum obtainable signal output power, $P_s^{\max}$, is set by the quantum efficiency:

$$P_s^{\max} = P_s^{\text{in}} + \frac{\lambda_p}{\lambda_s} P_p^{\text{in}} \tag{22}$$

where P_s^{in} is the signal input power and P_p^{in} is the input pump power.

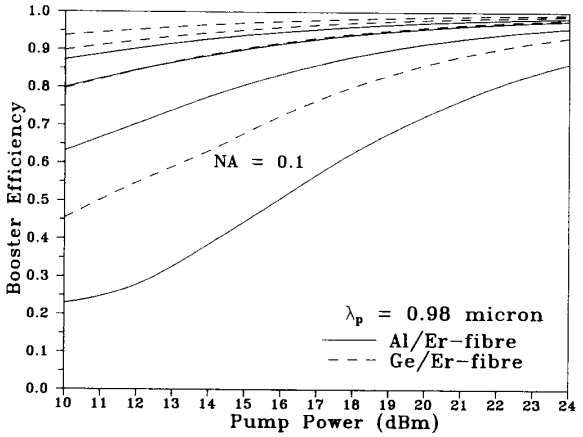

Fig. 8. Booster efficiency, i.e., the ratio between the number of signal output photons and the number of total input photons versus pump power in step-index Ge/Er-fibers (dashed) and Al/Er-fibers (solid), pumped at 0.98 μm. The signal input power is 1 mW. The numerical aperture (NA) is change from 0.1 to 0.4 in steps of 0.1.

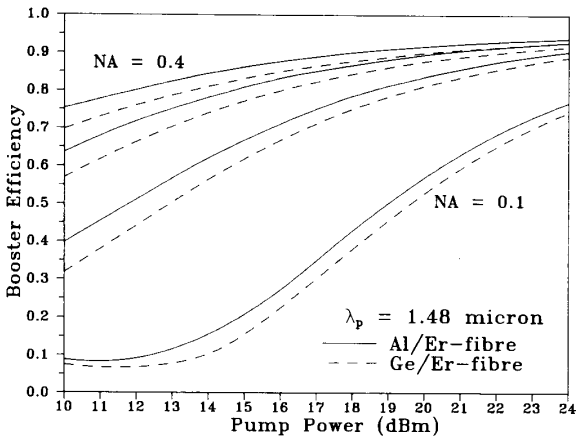

Fig. 9. Booster efficiency, i.e., the ratio between the number of signal output photons and the number of total input photons versus pump power in step-index Ge/Er-fibers (dashed) and Al/Er-fibers (solid), pumped at 1.48 μm. The signal input power is 1 mW. The numerical aperture (NA) is change from 0.1 to 0.4 in steps of 0.1.

When optimizing the booster amplifier, the goal is to convert as many pump photons into amplified signal photons. The following optimization will therefore be performed on the booster efficiency, η_b, defined as:

$$\eta_b = \frac{P_s(L)}{P_s^{\max}}. \tag{23}$$

In Figs. 8 and 9 the booster efficiency versus pump power for step-index erbium-doped fiber amplifiers with a signal input power of 1 mW is shown. Results for 0.98 μm (Fig. 8) and for 1.48 μm (Fig. 9) pumping of Ge/Er-fibers (dashed) as well as Al/Er-fibers (solid) are presented for NA = 0.1, 0.2, 0.3, and 0.4, the highest NA resulting in the highest efficiency. From Fig. 8 it is shown that the Ge/Er-fiber is more efficient than the Al/Er-fiber, when

pumping at 0.98 μm. For 1.48-μm pumping, see Fig. 9, the booster efficiency for the Al/Er-fiber is higher than the booster efficiency for the Ge/Er-fiber. However, the difference is not significant, and therefore it must be concluded, that the choice of codopant is not important, when pumping at 1.48 μm.

VIII. Conclusion

A comprehensive large-signal model for the erbium-doped fiber amplifier has been presented. The cross sections used by the model, has been determined experimentally for an erbium-doped fiber codoped with aluminum as well as for an erbium-doped fiber codoped with germanium. The model was used to design the index profile of erbium-doped fibers. When designing with regard to pump efficiency the optimum choice of profile is the step-index profile. The optimum cutoff wavelength was shown to be independent of the numerical aperture. For 0.98 μm and 1.48 μm the optimum cutoff wavelength is 0.80 and 0.90 μm, respectively. The highest pump efficiency was predicted for the Ge/Er-fibers pumped at 0.98 μm, where the maximum pump efficiency is 23 dB/mW, predicted for a numerical aperture of 0.4. This value is twice the value of 11 dB/mW for an Al/Er-fiber pumped at 0.98 μm.

The choice of codopants was shown not to be significant for the pump efficiency when pumping at 1.48 μm. The highest pump efficiency, for 1.48-μm pumping, was 8 dB/mW with a numerical aperture of 0.4.

For power booster amplifier applications, the results showed that the numerical aperture should be 0.20 or higher. The choice of codopant and pump wavelength was shown to be less significant for the efficiency of power amplifiers as compared to small signal amplifiers.

Acknowledgment

The authors would like to thank Dr. E. Nicolaisen for inspiring discussions.

Appendix A

In this appendix the two equations, (15) and (16), for the noise figure of an EDFA are derived.

When the signal propagates through the EDFA the signal-to-noise ratio (SNR) deteriorates, due to the stochastic nature of the interaction between the photons and Er^{3+}-ions. In the limit where an optical filter, with an infinitisimal bandwidth around the signal frequency, is applied at the output end of the EDFA, it can be shown [13] that the variance, V_s, of the signal power can be found by solving

$$\frac{dV_s(z)}{dz} = 2 \cdot [\gamma_e(\nu, z) - \gamma_a(\nu, z)]V_s(z) + [\gamma_e(\nu, z) + \gamma_a(\nu, z)]P_s(z) \quad \text{(A1)}$$

where the signal power, $P_s(z)$, is given as the solution to (13).

The noise figure, F, is defined, with respect to the idealized case of a coherent input signal ($V_s(0) = P_s(0)$), as the ratio between the SNR at the input and the SNR at the output

$$F = P_s(0) \cdot \frac{V_s(L)}{(P_s(L))^2}. \quad \text{(A2)}$$

By the use of (13) and (A1), (A2), F can be found from:

$$F = \int_0^L \frac{\gamma_e(\nu_s, z) + \gamma_a(\nu_s, z)}{P_s(z)} \cdot P_s(0)\, dz + 1. \quad \text{(A3)}$$

The noise figure is closely related to the spectral density of the forward traveling ASE. To show this, it is convenient to define the quantity, $p(z)$

$$p(z) = h\nu_s \cdot \left(\frac{V_s(z)}{P_s(z)} - 1\right). \quad \text{(A4)}$$

By the use of (13) and (A1) a differential equation for $p(z)$ can be obtained as

$$\frac{dp(z)}{dz} = h\nu_s \cdot \frac{V_s(z)}{P_s(z)} \cdot \frac{d}{dz}\left[\log_e\left(\frac{V_s(z)}{P_s(z)}\right)\right] \quad \text{(A5)}$$

which accordingly gives

$$\frac{dp(z)}{dz} = h\nu_s \cdot \frac{V_s(z)}{P_s(z)}[\gamma_e(\nu, z) - \gamma_a(\nu, z)]V_s(z) + h\nu_s \cdot [\gamma_e(\nu, z) + \gamma_a(\nu, z)]. \quad \text{(A6)}$$

By the use of (A4), (A6) finally leads to

$$\frac{dp(z)}{dz} = [\gamma_e(\nu, z) - \gamma_a(\nu, z)] \cdot p(z) + 2h\nu_s \cdot \gamma_e(\nu, z). \quad \text{(A7)}$$

Comparing with (10), it is seen that $p(z)$ and $S^+_{ASE}(\nu, z)$ obey the same differential equation and since both quantities vanish at $z = 0$, the following identity is derived:

$$S^+_{ASE}(\nu_s, L) = p(L) = h\nu_s \cdot \left(\frac{V_s(L)}{P_s(L)} - 1\right) \quad \text{(A8)}$$

which leads, see (A2), to the following relation between the noise figure, the gain and the forward ASE power spectral density at the signal frequency:

$$F = (S^+_{ASE}(\nu_s, L)/h\nu_s + 1)/G. \quad \text{(A9)}$$

References

[1] C. J. Koester and E. Snitzer, "Amplification in a fiber laser," *Appl. Opt.*, vol. 3, no. 10, p. 1182, 1964.

[2] C. R. Giles, E. Desurvire, J. L. Zyskind, and J. R. Simpson, "Noise performance of erbium-doped fiber amplifier pumped at 1.49 μm, and application to signal preamplification at 1.8 Gbits/s," *Photon. Technol. Lett.*, vol. 1, no. 11, pp. 367–369, 1989.

[3] Y. Kimura, K. Suzuki, and M. Nakazawa, "46.5 gain in Er^{3+}-doped fibre amplifier pumped by 1.48 μm GaInAsP laser diodes," *Electron. Lett.*, vol. 25, no. 24, pp. 1656–1657, 1989.

[4] M. Yamada *et al.*, "Er^{3+}-doped fiber amplifier pumped by 0.98 μm laser diodes," *Photon. Technol. Lett.*, vol. 1, no. 12, pp. 422–424, 1989.

[5] E. Desurvire, C. R. Giles, J. R. Simpson, and J. L. Zyskind, "Efficient erbium-doped fiber amplifier at $\lambda = 1.53$ μm with high output saturation power," *Proc. Cleo'89*, 1989, paper PD20.
[6] C. R. Giles, E. Desurvire, J. R. Talman, J. R. Simpson, and P. C. Becker, "2-Gbit/s signal amplification at $1 = 1.53$ μm in an erbium-doped single-mode fiber amplifier," *J. Lightwave Technol.*, vol. 7, no. 4, p. 651, 1989.
[7] C. R. Giles, E. Desurvire, J. R. Talman, and J. R. Simpson, "Transient gain and crosstalk in erbium-doped fiber-amplifiers," *Opt. Lett.*, vol. 14, no. 16, p. 880, 1989.
[8] R. I. Laming, S. B. Poole, and J. E. Tarbox, "Pump excited-state absorption in erbium-doped fibers," *Opt. Lett.*, vol. 13 p. 1084, 1988.
[9] Y. Kimura, K. Suzuki, and M. Nakazawa, "High gain erbium-doped fiber amplifier pumped in the 0.8 μm pump band," in *Proc. ECOC'90*, 1990, pp. 103–106.
[10] J. L. Zyskind, D. J. DiGiovanni, J. W. Sulhoff, P. C. Becker, and C. H. Brito Cruz, "High performance erbium-doped fiber amplifier pumped at 1.48 μm and 0.97 μm," in *Proc. OAA'90*, 1990, Post deadline paper, no. PDP6.
[11] M. Nakazawa, Y. Kimura, and K. Suzuki, "An ultra-efficient erbium-doped fiber amplifier of 10.2 dB/mW at 0.98 μm pumping and 5.1 dB/mW at 1.48 μm pumping," in *Proc. OAA'90*, 1990, Post deadline paper, no. PDP1.
[12] M. Shimizu, M. Yamada, H. Horiguchi, T. Takeshita, and M. Okayasu, "Erbium-doped fibre amplifiers with an extremely high gain coefficient of 11.0 dB/mW," *Electron. Lett.*, vol. 26, no. 20, pp. 1641–1643, 1990.
[13] K. Shimota, H. Takahasi, and C. H. Townes, "Fluctuations in amplification of quanta with application to maser amplifiers," *J. Physical Soc. Japan*, vol. 12, no. 6, pp. 686–700, 1957.
[14] H. Vendeltorp-Pommer, B. Pedersen, A. Bjarklev, and J. H. Povlsen, "Noise and gain performance for an Er^{+3} doped fibre amplifier pumped at 980 nm or 1480 nm," in *Proc. SPIE'90*, vol. 1373, 1990, paper no. 25.
[15] J. N. Sandoe, P. H. Sarkies, and S. Parke, "Variation of Er^{+3} cross section for stimulated emission with glass composition," *Appl. Phys.*, vol. 5, pp. 1788–1799, 1972.
[16] W. L. Barnes, R. I. Laming, and P. R. Morkel, "Absorption-emission cross-section ratio for Er^{3+} doped fibers at 1.5 μm," in *Proc. Cleo'90*, 1990, Paper no. JTUA3.
[17] K. Dybdal, N. Bjerre, J. E. Pedersen, and C. C. Larsen, "Spectroscopic properties of Er-doped silica fibers and preforms," in *Proc. SPIE'89*, 1989, pp. 209–218.
[18] B. Pedersen *et al.*, "Detailed theoretical and experimental investigation of high-gain erbium-doped fiber amplifier," *Photon. Technol. Lett.*, vol. 2, no. 12, 1990, pp. 863–865, 1990.
[19] P. L. Danielsen, "Analytical expressions for group delay in the far field from an optical fibre having an arbitrary profile," *J. Quantum Electron.*, vol. 19, p. 850, 1981.

*

Bo Pedersen was born in Roskilde, Denmark, on October 8, 1965. In August 1989 he received the M.Sc. degree in electrical engineering from the Electromagnetics Institute, Technical University of Denmark. In his Master thesis project he developed a three-dimensional BPM-model for the lens-ended fiber tapers. On February 1, 1990, he began work his Ph.D. degree on active optical waveguides at the Electromagnetics Institute. He is spending the year 1991 at GTE Laboratories, Waltham, MA, doing research on rare-earth-doped fiber amplifiers.

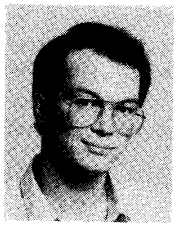

Anders Bjarklev was born in Roskilde, Denmark on July 2, 1961. He received the M.Sc. degree in electrical engineering from the Electromagnetics Institute, Technical University of Denmark, Lyngby in September 1985. He also received the Ph.D. degree from the Technical University of Denmark, Lyngby in June 1988.

He is presently employed as an Assistant Professor at the Electromagnetics Institute, Technical University of Denmark. His research interests are primarily within the field of characterization of active and passive optical waveguides.

*

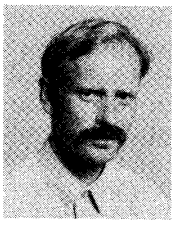

Jørn Hedegaard Povlsen received the M.Sc degree in physics from the H. C. Ørsted Institute of Copenhagen, Denmark in 1982.

In 1983 he joined the Electromagnetics Institute, Technical University of Denmark as an Associate Researcher. His research interests are in the field of characterization of active and passive optical waveguides and in the field of MQW structures.

*

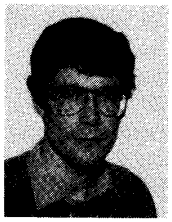

Kristen Dybdal received the Ph.D. degree in experimental atomic and nuclear physics from the University of Aarhus, Denmark, in 1980.

After a year at SUNY at Stony Brook, New York, he returned to the University of Aarhus, where he became an Assistant Professor. In 1987 he joined Jutland Telephone, where he is currently engaged in research on rare-earth doped fibers.

*

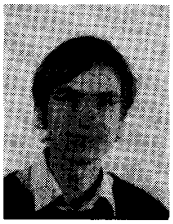

Carl Christian Larsen was born in Copenhagen, Denmark in 1958. He received the M.Sc. and the Ph.D. degrees in physics from the University of Copenhagen in 1984 and 1987, respectively.

In 1987 he joined the R&D department of LYCOM A/S with development of single-mode fibers and specialty fibers. His current interests are development and fabrication of rare-earth doped fibers.